Food Research International 89 (2016) 439–447

Contents lists available at ScienceDirect

Food Research International

journal homepage: www.elsevier.com/locate/foodres

Key role of collagen fibers orientation in casing-meat adhesion

Shuang Yang, Jinfeng Wang, Yuanliang Wang, Yanfeng Luo *

Key Laboratory of Biorheological Science and Technology (Chongqing University), Ministry of Education, Chongqing, 400030, China
Research Center of Bioinspired Materials Science and Engineering, College of Bioengineering, Chongqing University, Chongqing 400030, China

ARTICLE INFO

Article history:
Received 8 May 2016
Received in revised form 23 August 2016
Accepted 25 August 2016
Available online 28 August 2016

Keywords:
Collagen casing
Meat adhesion
Fiber orientation
Free shrinkage
Shrink force

ABSTRACT

Meat adhesion of collagen casings is important for the quality of sausages. In view of the crucial role of surface morphology in material adhesion, we hypothesize that the fiber orientation of collagen casings controls the meat adhesion. To verify this hypothesis, the casing-meat adhesion of four manufactured collagen casings (MCCs) was examined by the visual observation and the peeling force detection. The corresponding fiber orientation was investigated by using scanning electric microscope (SEM) and tensile tests. The results showed that MCC1 and MCC2 which had narrower directionality peak (−20° to −40° and −20° to 40°, respectively) and higher axial (σ_a) to radial (σ_r) strength ratios (1.90 ± 0.07 and 1.31 ± 0.02, respectively) demonstrated lower peeling forces than MCC3 and MCC4, indicating that a more isotropic structure is advantageous to the casing-meat adhesion. Further detection of the radial and axial shrink (including free shrinkage (S_r, S_a) and shrink force (F_r, F_a)) and observation of the local meat-casing interfaces by hematoxylin and eosin (HE) staining showed that appropriate S_r (15%–20%) and F_r (0.2–0.4 N) values at 80 °C helped to make the sausage tight whereas high F_a (>0.7 N) promoted the peeling off of the casings from meat. These results imply that an isotropic structure leads to balanced radial and axial shrink of MCCs, which may enhance the casing-meat adhesion. Overall, controlling a uniform fiber orientation should be an effective way to enhance the meat adhesion of collagen casings. Besides, shrinking properties should be efficient indicators for the meat adhesion of collagen casings.

1. Introduction

Collagen casings, as one of the most common artificial casings, possess many advantages over natural casings, including more uniform size and shape, and higher strength and flexibility to withstand rigor stuffing conditions (Harper, Barbut, Lim, & Marcone, 2013). Therefore, they can be highly automated to reduce the risk of contamination as often encountered by natural casings (Barbut, 2010). In addition, collagen casings are edible with tenderness and moisture permeability comparable to natural casings, being regarded as the best alternative to natural casings (Osburn, 2002; Simelane & Ustunol, 2005). Since the invention of collagen casings in the 1920s, most efforts have been focused on the development or modification of production process, apparatus and collagen dough formulations together with an attempt to regulate the casing thickness, caliber, mechanical properties (Bakker, Houben, Koolmees, Bindrich, & Sprehe, 1999; Harper, Barbut, Lim, & Marcone, 2012; Simelane & Ustunol, 2005), barrier properties (Amin & Ustunol, 2007) or sensory properties (Aleson-Carbonell, Fernandez-Lopez, Perez-Alvarez, & Kuri, 2005; Ledesma, Laca, Rendueles, & Díaz, 2016). However, few researches have been reported on the meat adhesion of collagen casings, regardless of the mechanism to control the casing-meat adhesion. In fact, the casing-meat adhesion is a more important property of collagen casings, which directly affects the quality attributes of sausages, especially for boiled sausages.

In the casing-meat system, the tumbling exudates of meat batter act as an adhesive to bind meat to the inner surface of collagen casings. Accordingly, the compositions of the meat batter influence the meat adhesion to collagen casings. It is reported that the exudates of muscle surface during the tumbling process are composed primarily of 80% water, 10–14% proteins and 0.2–5% lipids (Kerry, Stack, & Buckley, 1999), while the meat batter contains 68–70% water, 16–20% protein and 2–4% lipids (Ali et al., 2011; Yang et al., 2009). In addition, the thermal gelation of proteins in the exudates (mainly myofibrillar and sarcoplasmic protein) and the content of salts are believed to influence protein-protein interactions (Bombrun, Gatellier, Carlier, & Kondjoyan, 2014; Macfarlane, Schmidt, & Turner, 1977). Despite the obvious effects of meat batter on meat adhesion, desirable collagen casings should be able to circumvent or shun the contribution of meat batter and demonstrate good meat adhesion for a wide range of meat batter compositions. Unfortunately, the meat adhesion of many commercially manufactured collagen casings depends too much on the compositions of meat batter.

Regarding the effect of collagen casings on meat adhesion, the inner surface of collagen casings directly contacts with the exudates of meat batter so that its morphology should theoretically influence the meat

* Corresponding author: College of Bioengineering, Chongqing University (Campus A), Chongqing 400030, China.
E-mail address: yfluo@cqu.edu.cn (Y. Luo).

http://dx.doi.org/10.1016/j.foodres.2016.08.035
0963-9969/

adhesion. The morphology of collagen casings is controlled by manufacturing process. Generally, collagen casings are produced through extrusion of collagen dough by means of different types of extrusion cones (independently counter-rotating cones or one rotating cone) (Barbut, 2010; Hoogenkamp et al., 2015; Kobussen, Kobussen, Kobussen, & Smulders, 2001; Ziolko, 1979). Modulation of cone speeds may control the orientation of collagen fibers and thus the inner surface morphology (Hoogenkamp et al., 2015). The orientation of fibers has obvious influence on interfacial adhesion. For instance, random collagen-chitosan-thermoplastic polyurethane (TPU) nanofibers are more beneficial to cell adhesion compared to aligned fibers (Huang et al., 2011), and the orientation of muscle fibers has a significant effect on the binding strength of meat with myosin (Purslow, Donnelly, & Savage, 1987). Accordingly, the orientation of collagen fibers might be an important factor to regulate the meat adhesion of collagen casings. Moreover, collagen fibers will shrink along fiber orientation when heated in humidified atmosphere or hot water (Chahine, 2000; Su et al., 2012; Zhang, Ding, Chen, & Huang, 2014). For collagen casings, the shrinkage includes axial and radial shrinkage, whose magnitude is dependent on the fiber orientation. Imaginably, the shrinkage, particularly the axial shrinkage facilitates the separation of adherent casing-meat, though appropriate shrinkage is necessary for fullness of cooked sausages (Delius, 2005; Seiler, 1964).

In this respect, the aim of the present study was to explore the contributions of fiber orientation to the shrinkage of collagen casings and further to the casing-meat adhesion. The obtained results may provide a fundamental understanding on the meat adhesion of collagen casing involving collagen fiber orientation and shrinkage, which would be helpful in designing and manufacturing desirable collagen casings.

2. Materials and methods

2.1. Materials

According to our preliminary work, four commercially manufactured collagen casings (MCCs), denoted as MCC1 (Ø 19 mm), MCC2 (Ø 21 mm), MCC3 (Ø 23 mm), MCC4 (Ø 23 mm), were chosen to represent a range of typical orientations of collagen fibers. MCC1 and MCC2 were manufactured by China yet MCC3 and MCC4 by DEVRO (Scotland, England) and CORIA (South Carolina, USA). The protein content and water content of the four MCCs were all ca. 60% and 17% (Table S1), respectively. To eliminate the effects of different diameter, casings were axially sectioned and cut into identical strips for the subsequent tests.

2.2. Sausage preparation

Various sausages with a length of 5–6 cm were prepared by stuffing the commercial meat batter into casings by means of a sausage filler at 25 °C (MEITE, China). Six linked sausages were considered as one unit. The two endings of each unit were fastened by thread while the middle sections were divided by twisting. At least 18 sausages were prepared in each trial for each type of collagen casing.

The commercial meat batter was produced as follows: lean pork (40%), pork back fat (20%) and chicken breast (40%) obtained from the local supermarket were ground by a mincing machine through a 1.5 mm plate. Then the ground meat (500, in a unit of g/kg meat batter, the same below), water (350), soy protein (75) and the commercial seasoning and binder ingredients (75, mainly containing corn starch, NaCl, dextrose, sodium tripolyphosphate, sodium pyrophosphate, sodium hexametaphosphate, carrageenan, monosodium glutamate and monascus red) were mixed thoroughly in a mixer (about 30 min, 1000 r/min, Climax, China). The final meat batter was obtained by comminuting the mixture in a bowl chopper at high speed (3000 r/min, 5 min, Runyang ZB-40, China) to further reduce the particle size.

2.3. Meat adhesion test

Before the meat adhesion test, the sausages were dried at 60 °C for 20–30 min to remove the water on casing surfaces, and then the sausages were immersed in hot water (80 ± 2 °C) for 12 min to ensure the core temperature of sausages reaching 72 °C (Feng, Drummond,

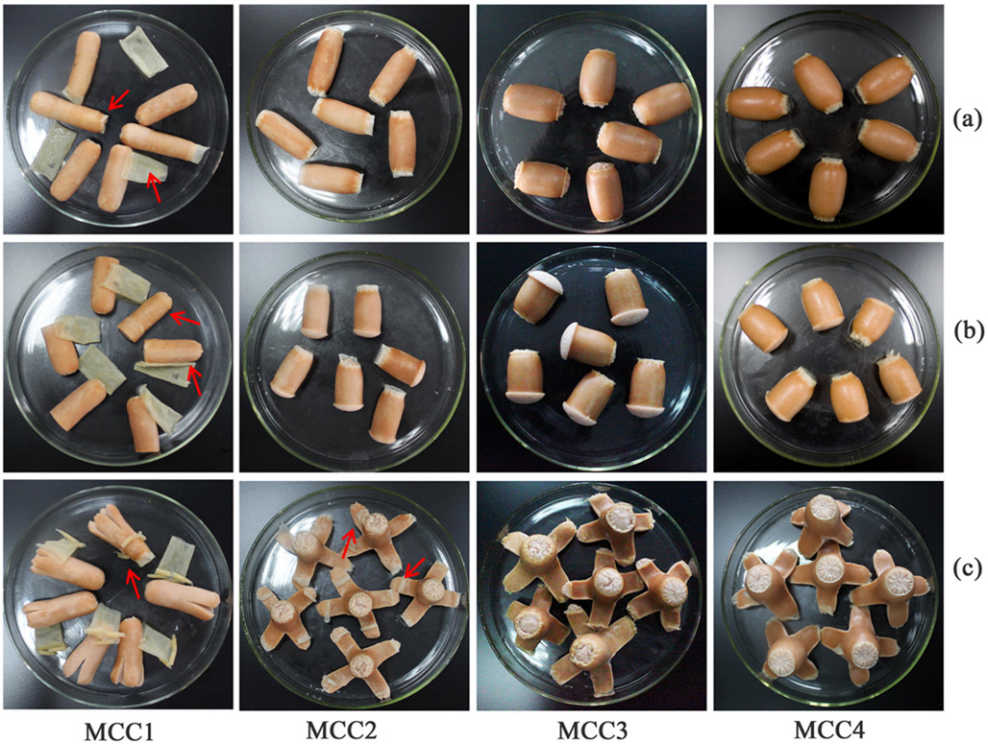

Fig. 1. Pictures showing the casing-meat adhesion of various MCCs after cooked in boiled water. (MCC1 (Ø 19 mm, China), MCC2 (Ø 21 mm, China), MCC3 (Ø 23 mm, DEVRO, England), MCC4 (Ø 23 mm, CORIA, USA)). (a) as filled sausages without any disposal; (b) sausages with a cut-off end (approximately 2 cm); (c) sausages with a cross-cut end (approximately 2 cm).

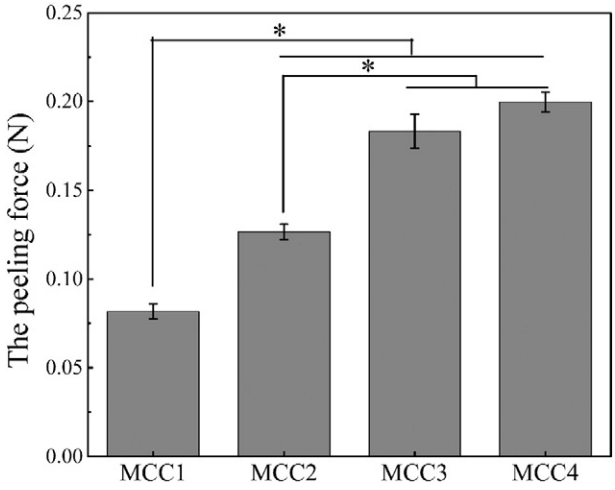

Fig. 2. The peeling force of various MCCs. The data are represented by the average of 60 points in the mid-section of peeling force-displacement curves and expressed as the means ± SEM ($n = 15$), * denoted $p < 0.05$.

Zhang, & Sun, 2014; Liu & Lanier, 2016). Thereafter, the sausages were stored in polyethylene bags at −20 °C overnight.

2.3.1. Visual observation

To visually observe the meat adhesion, six cooled sausages were cut off with the end (approximately 2 cm) to eliminate the artificial factors of unfullness, six were made with a cross-cut (approximately 2 cm) on the terminal to release radial pulling, and the rest were subjected to no disposal. Then the sausages were cooked by immersing into boiling water for 5 min and then pictured to observe whether the casings were separated from the meat.

2.3.2. Detection of the peeling force of MCCs

The casing-meat adhesion was further quantified by using a home-made instrument (Fig. S1) based on the method of peeling force (Rosinskin, Barmore, Dick, & Acton, 1989). The instrument is mainly composed of a temperature control system, a sub-division stepper motor drive, a lifting system, a control panel, a universal adjustable sample clamp, a pull/push dynamometer (0.01 N accuracy), and a data acquisition module that could be connected to a computer. Before testing, the samples were cut into a cuboid-like shape (60 mm in length, 10 mm in width, and 5 mm in thickness). Then the meat surface was adhered onto an aluminum plate (80 mm × 12 mm) by using Loctite type 409 cyanoacrylate glue (Peter, Donnelly, & Savage, 1987) and equilibrated to 25 °C. The aluminum plate was fixed on the lower clamp yet one end of the casing was fixed on the upper movable load-clamp. With the rising of the upper load-clamp at a velocity of 500 mm/min, the casing was peeled upward from the meat surface at an angle of 180° and the peeling force curve against displacement was recorded. The reported peeling force was represented by the average of 60 points in the mid-section of peeling force-time curves.

2.3.3. HE staining of the casing-meat interface

In order to understand how collagen fibers orientation influences the casing-meat adhesion, the microstructure of the casing-meat interface was visualized by using hematoxylin and eosin (HE) staining (He et al., 2014; Zhang et al., 2015). Briefly, the cross sections (0.5 cm in thickness) of the cooked sausages (showing casing-meat interface) were prefixed in 4% neutral buffered formalin for 24 h at room temperature and then dehydrated with ethanol. Following dehydration, the samples were embedded in paraffin wax, cut into sections (5 μm in thickness) and stained with HE. Three randomly selected visual fields of each section were examined under a light microscope (Olympus, Japan).

2.4. Observation of the orientation and morphology of collagen fibers

Various MCCs were placed in desiccators containing silica gel (25 °C) for 5–7 days and then fixed in objective tables using conductive tapes.

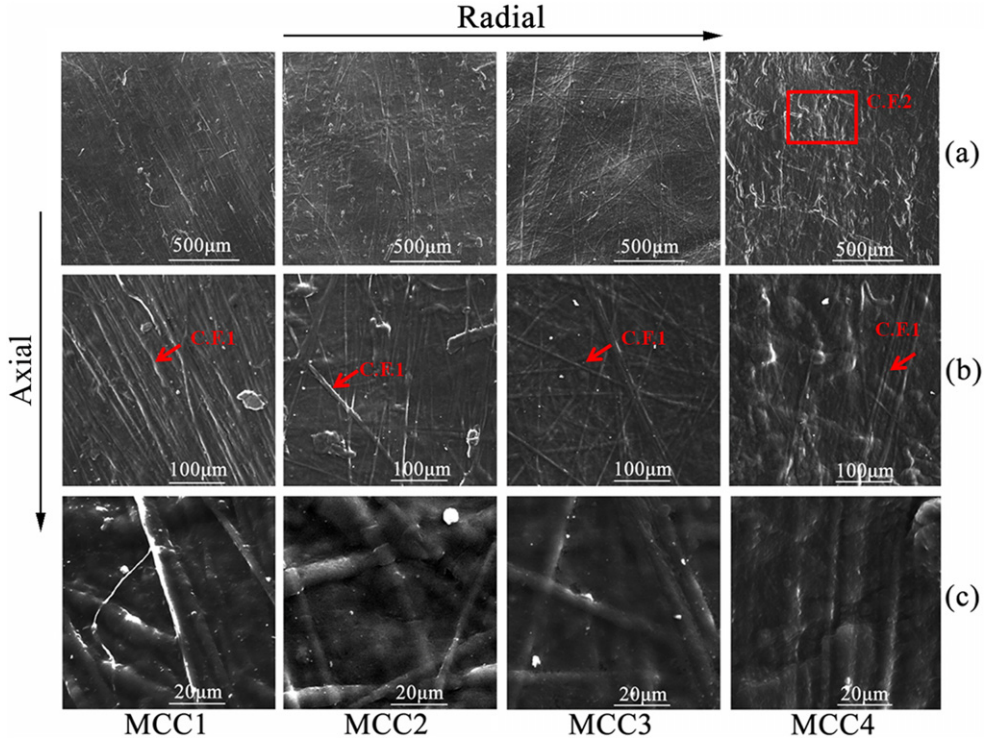

Fig. 3. The SEM images of collagen fibers in various MCCs. (C.F.1 = linear and spindly fibers; C.F.2 = random bending fibers). (a) ×100; (b) ×400; (c) ×2000.

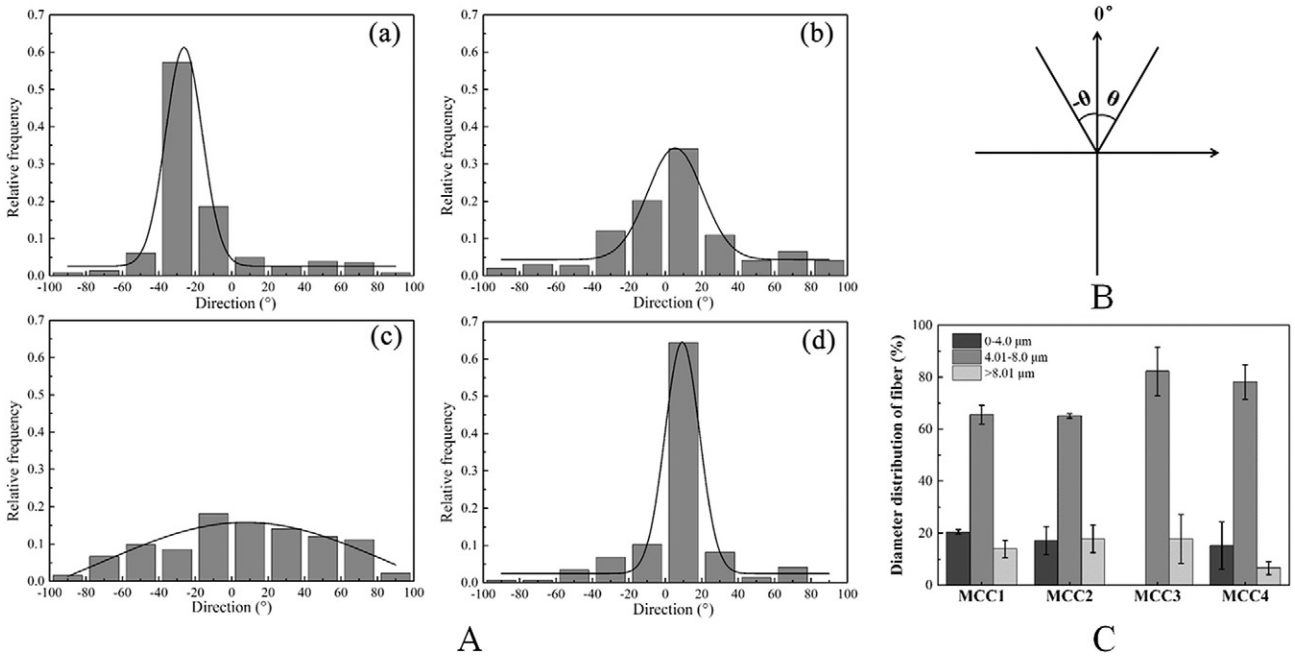

Fig. 4. Statistical analysis of the SEM images in Fig. 3. (A) The direction of collagen fibers in MCC1 (a), MCC2 (b), MCC3 (c), and MCC4 (d). The curves were fitted with a Gaussian curve. (B) Definition of the fibers' direction. Axial direction of casing was defined as 0°, clockwise angle to axial direction was defined as θ and counterclockwise angle was defined as −θ. (C) The diameter distribution of collagen fibers in various MCCs. Note: MCC4 contains both highly oriented and random fibers. The plotted fiber orientation and diameter were only based on the oriented fibers.

The fixed samples were conditioned for 48 h at 50 ± 3% relative humidity and 25 ± 2 °C and then coated with gold. The coated samples were observed under a scanning electron microscope (TESCAN VEGA 2, Czech Republic) at 10 kV. To further quantify the orientation of collagen fibers, the angles between the fiber and the casing axis were measured and the directionality peak was plotted by using Image J software.

2.5. Tensile mechanical properties

The tensile stress-strain curves were recorded using Electro Force 3330 (Bose, USA) according to method ASTM D 882–02 (ASTM, 2012). Before tests, the strip-shaped casings (55 mm × 10 mm) were conditioned for 48 h at 50 ± 3% relative humidity and 25 ± 2 °C. The initial distance of separation and loading velocity were fixed at 35 mm and 0.2 mm/s, respectively. The tensile strength (TS) was represented by the stress at film rupture. The reported data were the mean ± SEM ($n = 9$).

Meanwhile, the thickness of conditioned MCCs was measured with a coating thickness gauge (0.1 μm accuracy, SMART SENSOR AR930, HK).

Table 1
The radial and axial tensile mechanical properties of various MCCs.

	Radial tensile		Axial tensile			
	σ_b(r) (MPa)	ε_b(r) (%)	σ_b(a) (MPa)	ε_b(a) (%)	σ_b(a)/σ_b(r)	Thickness (μm)
MCC1	28.50 ± 1.38 ^{ac}	39.16 ± 4.00 ^{ab}	53.92 ± 0.84 ^{a}	23.86 ± 1.71 ^{a}	1.90 ± 0.07 ^{a}	49.72 ± 0.49 ^{a}
MCC2	36.82 ± 0.39 ^{b}	32.67 ± 1.08 ^{ab}	48.89 ± 0.19 ^{b}	30.60 ± 0.51 ^{ab}	1.31 ± 0.02 ^{b}	44.86 ± 0.68 ^{b}
MCC3	31.75 ± 0.07 ^{ab}	27.17 ± 0.32 ^{a}	33.16 ± 0.74 ^{c}	22.10 ± 2.69 ^{a}	1.06 ± 0.02 ^{c}	38.86 ± 0.42 ^{c}
MCC4	24.57 ± 2.24 ^{c}	41.45 ± 4.04 ^{b}	29.42 ± 1.31 ^{c}	34.56 ± 2.59 ^{b}	1.29 ± 0.03 ^{b}	46.45 ± 0.57 ^{b}

σ_b: strength at break; ε_b: strain at break. The data are expressed as the means ± SEM, $n = 9$ for tensile mechanical testing and $n = 30$ for thickness testing.

The mean thickness of five measurements for each specimen was employed for stress calculation.

2.6. Detection of the free shrinkage ratio of MCCs

The free shrinkage ratios were determined by measuring length change ratios (radial and axial) of the strip-shaped samples (30 mm × 100 mm) before and after immersion in water at various temperatures (60 °C, 80 °C, 100 °C) for 2 min. The reported data were the mean ± SEM ($n = 15$).

2.7. Detection of the shrink force of MCCs

The shrink force-time curves were recorded by using the same instrument for peeling force. To test the shrink force, the two ends of strip-shaped samples (55 mm × 10 mm) were fixed with medical proof fabrics for slide prevention and then immersed in water at various temperatures (60 °C, 80 °C, 95 °C) for 3 min. Selection of 95 °C instead of 100 °C is to eliminate the disturbance of boiled water to the detected shrink force. The initial separation distance and descent velocity were fixed at 35 mm and 60 mm/s, respectively. The reported forces were the maximum shrink force detected. The reported data were the mean ± SEM ($n = 15$).

2.8. Statistical analysis

All data were expressed as mean ± SEM. The Shapiro-Wilk test and Levence's test were used to check the normality distribution of data and the homogeneity of the variances, respectively. A general linear model was used for the analysis of one-way variance (ANOVA). The type of MCCs means and interactions were compared by Tukey's multiple comparison analysis and Bonferroni's test. These analyses were performed using software SPSS (SPSS Statistics 20, IBM, USA). Test statistics were regarded as significant when p was ≤0.05.

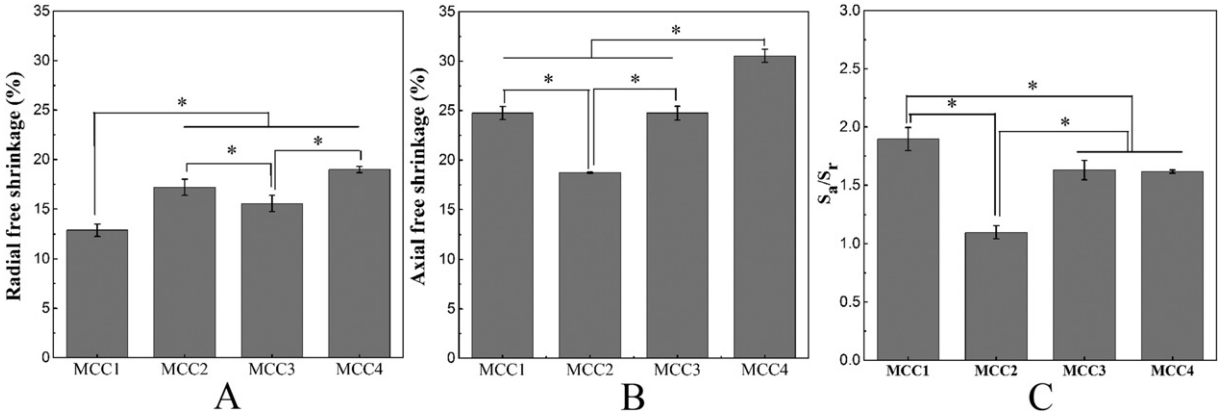

Fig. 5. The free radial (A, S_r) and axial (B, S_a) shrinkage of MCCs in water at 80 °C, together with the corresponding ratios of S_a to S_r at 80 °C (C, S_a/S_r). The data are expressed as the means ± SEM ($n = 15$), * denoted $p < 0.05$.

3. Results and discussion

3.1. Casing-meat adhesion

The visual meat adhesion of various MCCs was shown in Fig. 1. The adhesion of MCC2, MCC3 and MCC4 was significantly better than that of MCC1. Specifically, MCC3 and MCC4 demonstrated complete meat adhesion for all sausages. Sound meat adhesion with MCC2 was observed as well for the as-filled and end-cut sausages, though partial separation of casings from the meat was observed at the end of cross-cut sausages. In contrast, MCC1 casings obviously separated from the meat for all sausages. Furthermore, excessive radial and axial shrinkage was observed (Fig. 1a–c-MCC1). Meanwhile, the peeling force was quantified according to the peeling force-time curves (Fig. S2). The results (Fig. 2) indicated that MCC3 and MCC4 had obviously higher peeling forces than MCC1 and MCC2 ($p < 0.05$), presenting a pattern of MCC3 ≈ MCC4 > MCC2 > MCC1. Therefore, it may be concluded that the casing-meat adhesion presents an order of MCC1 < MCC2 < MCC3 ≈ MCC4. To guide the fabrication of casings with sound casing-meat adhesion, it is essentially important to find the parameters which control the differential casing-meat adhesion. Unfortunately, little attention has been paid to the meat adhesion of collagen casings, though the meat adhesion of cellulose-based casings has been extensively studied by applying a coating to the inner surface of cellulose casings (Blumenberg, Henze-wethkamp, & Neuschulz, 2013; Garcia Martinez, 2014; Hammer, Kuenzel, & Effern, 2011).

3.2. The orientation and morphology of collagen fibers

The adhesion of two polymer materials is mainly attributed to the intermolecular and interatomic interactions at the interface of their surfaces (Poisson, Hervais, Lacrampe, & Krawczak, 2006), which has been known to depend on the surface characteristics of materials. Therefore, we hypothesized that the collagen fibers orientation of casings should be a key parameter to influence the casing-meat adhesion. To verify this hypothesis, the surface texture of casings was detected and quantified.

Fig. 3 shows an overview of the collagen fibers of the inner surface of various MCCs. Two types of surface textures were observed. One was observed on MCC1, MCC2 and MCC3, where linear and spindle fibers interwove with different directions. In detail, the fibers of MCC1 extended mainly along one direction, resulting in an obviously anisotropic structure. Crisscross networks were observed on both MCC2 and MCC3, especially on MCC3. These structures were observed by other groups as well (Adzaly, Jackson, Kang, & Almenar, 2016; Harper et al., 2012; Ledesma et al., 2016). The other type of surface texture was observed on MCC4, which contained both aligned parallel fibers and random bending fibers. The parallel fibers were mainly aligned in the axial direction of casings.

The orientation of collagen fibers was further quantified by measuring the angle between the fiber and the casing axis according to Fig. 4B. The axial direction of casings was set as 0°, a clockwise angle from the fiber to the casing axial direction was defined as θ yet an anticlockwise

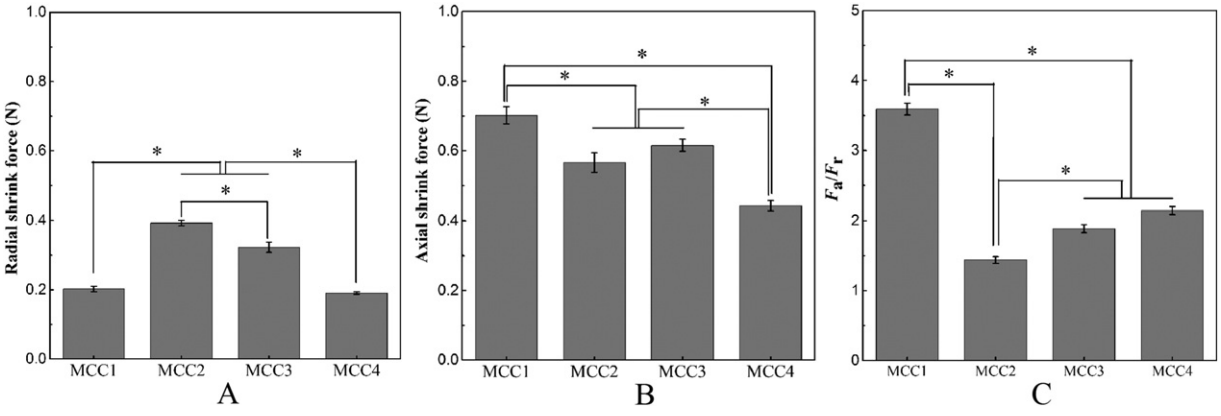

Fig. 6. The maximum radial (A, F_r) and axial (B, F_a) shrink force of MCCs in water at 80 °C, together with the corresponding ratios of F_a to F_r at 80 °C (C, F_a/F_r). The data are expressed as the means ± SEM ($n = 15$), * denoted $p < 0.05$.

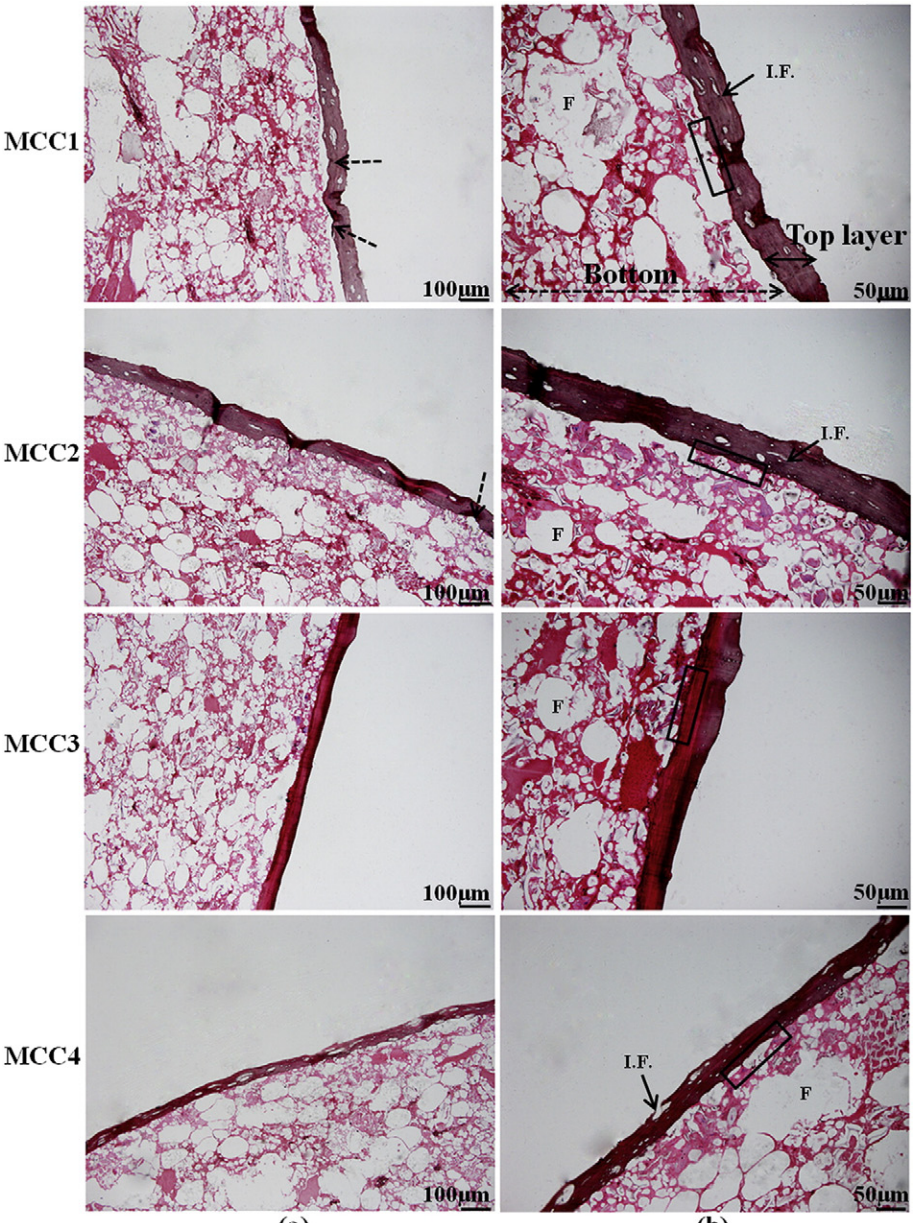
MCC1
MCC2
MCC3
MCC4
I.F.
F
Top layer
Bottom
100μm
50μm
(a)
(b)
A
The percentage of stained (%)
0
10
20
30
40
50
60
70
80
*
*
MCC1
MCC2
MCC3
MCC4
B

angle as − θ. The values of θ varied between 0° and 90°. In view of the existence of many random fibers in MCC4, MCC4 was excluded from the comparison of fiber orientation. As shown in Fig. 4A, the directionality peak of MCC1 was the narrowest and sharpest, followed by MCC2 and MCC3. Specifically, most of the angles in MCC1 were between −20° to −40°, suggesting that the fibers were mainly oriented along the casing axis direction while few were along the casing radial direction. Contrarily, in MCC3, the fiber orientation to the axial direction of casings was almost in balance with that to the radial direction, since the angles were almost evenly distributed. A wider directionality peak represents a more isotropic orientation (Hoogenkamp et al., 2015), hence, it could be concluded that the isotropy of MCCs follows an order of MCC1 < MCC2 < MCC3. This order is consistent with the order of casing-meat adhesion as shown in Figs. 1 and 2, verifying our hypothesis that the orientation and distribution of collagen fibers influence the casing-meat adhesion and an isotropic structure is more beneficial to meat adhesion. In fact, natural casings, which have perfect meat adhesion, are isotropic in texture as well (Harper et al., 2012; Ledesma et al., 2016). In addition, though MCC4 has a sharp directionality peak with a peak angle between 0°–20°, random fibers might increase the isotropy of fiber orientation, which leads to excellent meat adhesion of MCC4.

3.3. The tensile mechanical property

Hoogenkamp et al. (2015) reported that fibers' orientation has an obvious influence on the mechanical property of collagen films. In order to further verify the orientation and distribution of collagen fibers in various MCCs, the tensile mechanical property was measured. The thickness of MCCs was measured as well (Table 1) for tensile stress detection.

Considering that fiber diameter may affect the mechanical property of casings, the fiber diameters were measured from the SEM pictures (Fig. 4C). It is noted that the fiber diameters in all the four MCCs ranged from 4.01 μm to 8 μm, demonstrating insignificant differences in fiber diameters. Therefore, the fibers' orientation could be regarded as the main factor to influence the mechanical properties of MCCs.

The typical stress-strain curves of various MCCs are shown in Fig. S3, including both the radial (Fig. S3A) and axial (Fig. S3B) ones. The break strength (σ_b) and break strain (ε_b) were summarized in Table 1. All the σ_b and ε_b values of four MCCs, including both radial and axial ones were in a range of 24.57–53.92 MPa and 22.10–41.45%, respectively. Compared with 'gold standard' natural casings and other commercial collagen casings (Adzaly, Jackson, Villalobos-Carvajal, Kang, & Almenar, 2015; Amin & Ustunol, 2007; Bakker et al., 1999; Simelane & Ustunol, 2005), these σ_b and ε_b values were high enough to satisfy the automated filling requirements of sausages. In spite of this, the high area under the axial stress-strain curve of MCC1 corresponds to high toughness (Fratzl, 2008), potentially impairing the chewiness of MCC1.

To indicate the isotropy of MCCs, the ratios of axial σ_b ($\sigma_b(a)$) to the corresponding radial σ_b ($\sigma_b(r)$) were calculated as well (Table 1). Higher $\sigma_b(a)/\sigma_b(r)$ value means lower isotropy. There were significant differences ($p < 0.05$) among MCC1, MCC2 and MCC3. It can be seen that MCC1 had the highest $\sigma_b(a)/\sigma_b(r)$ value (1.90 ± 0.07), followed in turn by MCC2 (1.31 ± 0.02), MCC4 (1.29 ± 0.03) and MCC3 (1.06 ± 0.02). The order of isotropy based on $\sigma_b(a)/\sigma_b(r)$ values is consistent with that from SEM results for MCC1, MCC2 and MCC3 (Figs. 3 and 4). Regarding MCC4, no significant difference ($p > 0.05$) was observed between MCC2 and MCC4. Though axially aligned fibers were observed in MCC4 (Fig. 3), random fibers attenuated the negative contribution of axially aligned fibers to the isotropy, leading to low $\sigma_b(a)/\sigma_b(r)$ value and thus improved isotropy. In conclusion, the isotropy of MCCs based on $\sigma_b(a)/\sigma_b(r)$ values takes an order of MCC1 < MCC2 ≈ MCC4 < MCC3. It should be noted that this order is a little different from the order of meat adhesion (MCC1 < MCC2 < MCC3 ≈ MCC4). This minor divergence should be due to the fact that the tensile test does not reflect the thermal properties of collagen fibers which, however, are significantly involved in the meat adhesion.

3.4. The free shrinkage of MCCs

It is known that collagen fibers undergo shrinkage along the fiber orientation when suffered from a thermal denaturation (Budrugeac, Badea, Gatta, Miu, & Comanescu, 2010; Chahine, 2000; Savic & Savic, 2002). The thermal-induced shrinkage of collagen casings, on the other hand, is accompanied by meat expansion, thus playing a crucial role in controlling casing-meat adhesion. To further verify the reliance of casing-meat adhesion of MCCs on fiber orientation, the free radial and axial shrinkages in water at various temperatures were detected.

During sausage manufacturing, the filled sausages are generally dried at 60 °C and then steam-cooked at 80 °C (Feng et al., 2014; Harper et al., 2012). For boiled sausages, they are cooked at 100 °C water. Accordingly, 60 °C, 80 °C and 100 °C were selected to evaluate the free shrinkage of MCCs. As shown in Fig. S4A and B, the radial and axial free shrinkages of all MCCs increased with the increase of temperature from 60 °C to 80 °C. However, no significant difference ($p > 0.05$) was observed between 80 °C and 100 °C, implying that the thermal denaturation of collagen fibers was almost completed at 80 °C. Other researchers reported similar denaturation temperatures for proteins such as myosin, sarcoplasmic and connective proteins, which are partially denatured at 60 °C and completely denatured at 70–80 °C (Fernandez-Martin, Fernandez, Carballo, & Jimenez-Colmenero, 2000; Villamonte, Simonin, Duranton, Cheret, & Lamballerie, 2013). Taking account of the complete denaturation of casings at 80 °C and the fact that appropriate S_r value is good for casing-meat adhesion (Delius, 2005; Wallace, 1986), it is reasonably deduced that the S_r values at 80 °C should be the most crucial to casing-meat adhesion. The S_r values of various MCCs found that MCC1 had the lowest S_r values at 80 °C (Fig. 5A), supporting the correlation of low S_r (<15%) with the poor casing-meat adhesion of MCC1. The S_a/S_r ratios at 80 °C were further calculated (Fig. 5C), and they were 1.90 ± 0.10, 1.10 ± 0.04, 1.63 ± 0.08, 1.62 ± 0.01 for MCC1, MCC2, MCC3 and MCC4, respectively. MCC1 had the highest S_a/S_r ratio, suggesting the lowest isotropy as observed by SEM (Fig. 3) and tensile tests (Table 1). More importantly, when the S_a/S_r ratio was higher than 1.90, the axial shrinkage could overwhelm the radial shrinkage, potentially leading to axial deviation and promoting separation of casing from meat.

3.5. The shrink force of MCCs

The thermal denaturation of casings would not only result in shrinkage in size, but also produce shrink force (Delius, 2005). The former is associated with the fullness of sausages whereas the latter more directly affects the casing-meat adhesion. Therefore, the radial and axial shrink forces were detected in water at various temperatures. To eliminate the disturbance of water vapors to the detected shrink force, 95 °C rather than 100 °C was employed.

As shown in Fig. S6A and B, both the radial and axial shrink forces of MCCs constantly increased with the increase of temperature from 60 °C to 95 °C. Specially, the shrink forces at 80 °C were significantly lower ($p < 0.05$) than their corresponding forces at 95 °C. This phenomenon was divergent from the temperature-dependence of free shrinkages. Despite the divergent temperature-dependence, the ratios of F_a to the corresponding F_r at 80 °C (Fig. 6C) indicated similar isotropy of MCCs to that from the free shrinkage S_a/S_r, i.e. MCC1 < MCC4 ≈ MCC3 < MCC2 (Fig. 5C). It has been proved in this study that the shrink force of MCCs,

Fig. 7. (A) Light microscopy pictures of the cross sections of cooked sausages at 80 °C, indicating the interfaces of various MCCs with meat. (a) ×100; (b) ×200. (B) The ratio of interface length with HE stained color to the total interface length. F = extracted fat globule; I.F. = insoluble fibers. * denoted $p < 0.05$.

induced by the thermal denaturation of collagen fibers, was highly dependent on the fiber orientation. Theoretically, high F_r helps to make the sausage tight, increase the mechanical coupling and molecular bonding effects of the casing-meat interface and thus prevent separation of casings from meat (Awaja, Gilbert, Kelly, Fox, & Pigram, 2009). However, high F_a creates strong interfacial shear force, prevents the tumbling exudates from adhering well to the collagen fibers and thus helps to peel off the casings from meat (Kim & Netravali, 2010). Therefore, F_r can partially counteract the negative contribution of F_a to meat adhesion. For MCC1, fewer radially orientated fibers than axially orientated ones (Fig. 3, Fig. 4A) resulted in too weak F_r to counteract its high F_a (i.e. high F_a/F_r value) so that its meat adhesion was poor. Compared with MCC1, the fiber orientation in MCC3 was the most uniform, which produced a F_r value high enough to counterbalance the negative contribution of F_a, resulting in sound meat adhesion as observed in Fig. 1 and Fig. 2. Regarding MCC4, the randomly orientated fibers increased the uniformity of fiber orientation, resulting in comparable F_a/F_r with MCC3 (Fig. 6C) and good meat adhesion (Figs. 1 and 2). One exception was seen by MCC2 whose F_r was similarly high enough to counteract the F_a (low F_a/F_r) (Fig. 6C) yet the meat adhesion was not as good as MCC3 or MCC4 (Figs. 1 and 2). This might be due to its fastest F_a increase to the maximum value in <0.5 s (inset in Fig. S5B), when the gelatinization of meat batter has not well formed, adversely impacting the meat adhesion of MCC2. Further work should be done to clarify how the MCC orientation and other factors affect the shrinkage speed and the meat adhesion.

3.6. Microstructure of the casing-meat interface

During the process of cooking, heating induces the gelatinization of both tumbling exudates such as myofibrillar protein in meat batter and collagen fibers in collagen casings, promoting physical fusion of meat and casings at the casing-meat interface (Barbut, 2010; Bombrun et al., 2014). In addition, heating may initiate chemical reactions between meat and casing, which, together with the gelatinization-induced physical fusion, contributes to the casing-meat adhesion (Ioi, 2013). Myofibrillar protein and collagen can be stained as pink by HE staining (Rolf Schroder & Benedikt Schoser, 2009). Accordingly, HE staining was performed to visualize the casing-meat interface, which helps to understand how the collagen fibers orientation of collagen casings influences the casing-meat adhesion.

Fig. 7 shows the cross-sections of sausages stuffed into various MCCs, where the top layer (indicated by solid double arrows) is the casing and the bottom structure (indicated by dotted double arrows) is the meat batter. The empty holes (indicated by F) in the bottom structure represented fat globules that were removed by ethanol during dehydration prior to fixing samples. Those ribbon-like white areas in the top layer should be insoluble cellulose fibers (marked as I.F., indicated by solid arrows), which has been proved by the periodic acid–Schiff (PAS) staining of commercial collagen dispersions (Cranston & Gray, 2008; Ioi, 2013; Reddy & Yang, 2005). Similar microstructures were observed by Barbut et al. (Barbut, 2010; Harper et al., 2012) for other examples of collagen casings.

As shown in Fig. 7A, the interfaces between the casing and the meat (indicated by rectangle) were distinct for MCC1 and MCC2. In contrast, obvious fusion of meat into the casing was observed for MCC3 and MCC4, indicating better casing-meat adhesion compared to MCC1 and MCC2. In order to quantify the interfacial fusion, the ratio of interface length with HE stained color to the total interface length, expressed as percentage, was measured by using Image J software and shown in Fig. 7B. It should be noted that MCC1 had the lowest percentage while MCC3 and MCC4 had the highest with no significant difference ($p > 0.05$), suggesting that the casing-meat adhesion strength follows an order of MCC1 < MCC2 < MCC3 ≈ MCC4. This order is consistent with the order of casing-meat adhesion as shown in Figs. 1 and 2.

More importantly, local shrinkage took place in MCC1 and MCC2, especially in MCC1 (indicated by dotted arrows). This is in accordance with the results of shrink testing (Figs. 5, 6 and Fig. S5) and supports the hypothesis that adhesion separation might be due to a greater local shrinkage of casings before gelatinization, which impairs the adhesion strength between casings and meat.

4. Conclusion

We found, for the first time, that collagen fibers orientation and distribution have important influences on casing-meat adhesion. A more isotropic structure, that is, more uniform radial and axial orientation and distribution of collagen fibers is advantageous to the casing-meat adhesion. The potential mechanism appears to be that an isotropic structure leads to balanced radial and axial shrink (including free shrinkage and shrink force) of MCCs. Therefore, a consideration of fibers orientation when designing collagen casings would be helpful in improving the casing-meat adhesion. Moreover, radial and axial shrink (free shrinkage and shrink force) should be employed as a more efficient indicator for collagen fiber orientation and a predictor for casing-meat adhesion.

Acknowledgments

This work was supported by grants from the Fundamental Research Funds for the Central Universities (No. 106112015CDJZR238807) and the National Natural Science Foundation of China (No. 11532004 and No. 31370946).

Appendix A. Supplementary data

Supplementary data to this article can be found online at http://dx.doi.org/10.1016/j.foodres.2016.08.035.

Reference

Adzaly, N. Z., Jackson, A., Kang, I., & Almenar, E. (2016). Performance of a novel casing made of chitosan under traditional sausage manufacturing conditions. *Meat Science, 113*, 116–123.
Adzaly, N. Z., Jackson, A., Villalobos-Carvajal, R. V., Kang, I., & Almenar, E. (2015). Development of a novel sausage casing. *Journal of Food Engineering, 152*, 24–31.
Aleson-Carbonell, L., Fernandez-Lopez, J., Perez-Alvarez, J. A., & Kuri, V. (2005). Functional and sensory effects of fibre-rich ingredients on breakfast fresh sausages manufacture. *Food Science and Technology International, 11*, 89–97.
Ali, M. S., Kim, G. D., Seo, H. W., Jung, E. Y., Kim, B. W., Yang, H. S., & Joo, S. T. (2011). Possibility of making low-fat sausages from duck meat with addition of rice flour. *Asian-Australasian Journal of Animal Sciences, 24*, 421–428.
Amin, S., & Ustunol, Z. (2007). Solubility and mechanical properties of heat-cured whey protein-based edible films compared with that of collagen and natural casings. *International Journal of Dairy Technology, 60*, 149–153.
ASTM (2012). Standard test methods for tensile properties of thin plastic sheeting, D882-12. *Annual book of ASTM standards*. American Society for: Testing and Materials, Philadelphia (PA).
Awaja, F., Gilbert, M., Kelly, G., Fox, B., & Pigram, P. J. (2009). Adhesion of polymers. *Progress in Polymer Science, 34*, 948–968.
Bakker, W. A. M., Houben, J. H., Koolmees, P. A., Bindrich, U., & Sprehe, L. (1999). Effect of initial mild curing, with additives, of hog and sheep sausage casings on their microbial quality and mechanical properties after storage at difference temperatures. *Meat Science, 51*, 163–174.
Barbut, S. (2010). Microstructure of natural, extruded and co-extruded collagen casings before and after heating. *Italian Journal of Food Science, 22*, 126–133.
Blumenberg, K.D., Henze-wethkamp, H., & Neuschulz, W. (2013). Sausage skin with improved sausage meat adhesion. CaseTech GmbH & Co. KG, Bomlitz, DE. Patent No: EP 2,140,765 *B*1.
Bombrun, L., Gatellier, P., Carlier, M., & Kondjoyan, A. (2014). The effects of low salt concentrations on the mechanism of adhesion between two pieces of pork semimembranosus muscle following tumbling and cooking. *Meat Science, 96*, 5–13.
Budrugeac, P., Badea, E., Gatta, G. D., Miu, L., & Comanescu, A. (2010). A DSC study of deterioration caused by environmental chemical pollutants to parchment, a collagen-based material. *Thermochimica Acta, 500*, 51–62.
Chahine, C. (2000). Changes in hydrothermal stability of leather and parchment with deterioration: A DSC study. *Thermochimica Acta, 365*, 101–110.
Cranston, E. D., & Gray, D. G. (2008). Birefringence in spin-coated films containing cellulose nanocrystals. *Colloids and Surfaces A: Physicochemical and Engineering Aspects, 325*, 44–51.
Delius, U. (2005). Polyamide-based sausage skin which can be filled manually. Kalle Nalo GmbH & Co. KG, Wiesbaden, DE. Patent No: US 6,919,112.

Feng, C. H., Drummond, L., Zhang, Z. H., & Sun, D. W. (2014). Evaluation of innovative immersion vacuum cooling with different pressure reduction rates and agitation for cooked sausages stuffed in natural or artificial casing. *LWT- Food Science and Technology*, *59*, 77–85.

Fernandez-Martin, F., Fernandez, P., Carballo, J., & Jimenez-Colmenero, F. (2000). DSC study on the influence of meat source, salt and fat levels, and processing parameters on batters pressurisation. *European Food Research and Technology*, *211*, 387–392.

Fratzl, P. (2008). Collagen: Structure and mechanics, an introduction. In P. Fratzl (Ed.), *Collagen structure and mechanics* (pp. 1–12). New York: Springer Science.

Garcia Martinez, I.I. (2014). Shirring composition and used thereof. Viscofan, S.A., Navarra, ES. Patent No: EP 2,749,168 A1.

Hammer, K.D., Kuenzel, U., & Effern, V. (2011). Cellulose hydrate sausage casing featuring minimum meat cling. Kalle GmbH, Wiesbaden, DE. Patent No: US 7,968,161 B2.

Harper, B. A., Barbut, S., Lim, L. T., & Marcone, M. F. (2012). Microstructural and textural investigation of various manufactured collagen sausage casings. *Food Research International*, *49*, 494–500.

Harper, B. A., Barbut, S., Lim, L. T., & Marcone, M. F. (2013). Characterization of 'wet' alginate and composite films containing gelatin, whey or soy protein. *Food Research International*, *52*, 452–459.

He, S., Wang, G.L., Zhu, Y.Y., Wu, M.H., Ji, Z.G., Seng, J., Ji, Y., Zhou, J.M., & Chen, L. (2014). Application of the CellDetect® staining technique in diagnosis of humancervical cancer. Gynecologic Oncology, 132, 383–388.

Hoogenkamp, H. R., Bakker, G. J., Wolf, L., Suurs, P., Dunnewind, B., Barbut, S., ... Daamen, W. F. (2015). Directing collagen fibers using counter-rotating cone extrusion. *Acta Biomaterialia*, *12*, 113–121.

Huang, C., Chen, R., Ke, Q., Morsi, Y., Zhang, K., & Mo, X. (2011). Electrospun collagen-chitosan-TPU nanofibrous scaffolds for tissue engineered tubular grafts. *Colloids and Surfaces. B, Biointerfaces*, *82*, 307–315.

Ioi, M. A. (2013). *An investigation of commercial collagen dispersions and their use in co-extrusion sausage manufacturing.* Canada: University of Guelph (Chapter 3).

Kerry, J. F., Stack, F., & Buckley, D. J. (1999). The rheological properties of exudates from cured porcine muscle: Effects of added non-meat proteins. *Journal of the Science of Food and Agriculture*, *79*, 101–106.

Kim, J. T., & Netravali, A. N. (2010). Effect of protein content in soy protein resins on their interfacial shear strength with ramie fibers. *Journal of Adhesion Science and Technology*, *24*, 203–215.

Kobussen, P.J., Kobussen, J.J.J.P., Kobussen, M.W.H., & Smulders, F.G. (2001). Continuous food processing system, Townsend Engineering Company, Des Moines, IA, USA. Patent No: US 6,331,104 B1.

Ledesma, E., Laca, A., Rendueles, M., & Díaz, M. (2016). Texture, colour and optical characteristics of a meat product depending on smoking time and casing type. *LWT- Food Science and Technology*, *65*, 164–172.

Liu, R., & Lanier, T. C. (2016). Rapid (microwave) heating rate effects on texture, fat/water holding, and microstructure of cooked comminuted meat batters. *Food Research International*, *81*, 108–113.

Macfarlane, J. J., Schmidt, G. R., & Turner, R. H. (1977). Binding of meat pieces: A comparison of myosin, actomyosin and sarcoplasmic proteins as binding agents. *Journal of Food Science*, *42*, 1603–1605.

Osburn, W. N. (2002). Collagen casings. In A. Gennadios (Ed.), *Protein-based films and coatings* (pp. 445–465). Boca Raton, Fla.: CRC Press LLC.

Peter, P. P., Donnelly, S. M., & Savage, A. W. J. (1987). Variations in the tensile adhesive strength of meat-myosin junctions due to test configurations. *Meat Science*, *19*, 227–242.

Poisson, C., Hervais, V., Lacrampe, M. F., & Krawczak, P. (2006). Optimization of PE/binder/PA extrusion blow-molded films. II. Adhesion properties improvement using binder/EVA blends. *Journal of Applied Polymer Science*, *101*, 118–127.

Purslow, P. P., Donnelly, S. M., & Savage, A. W. J. (1987). Variations in the tensile adhesive strength of meat myosin junctions due to test configurations. *Meat Science*, *19*, 227–242.

Reddy, N., & Yang, Y. (2005). Properties and potential applications of natural cellulose fibers from cornhusks. *Green Chemistry*, *7*, 190–195.

Rolf Schroder, M. D., & Benedikt Schoser, M. D. (2009). Myofibrillar myopathies: A clinical and myopathological guide. *Brain Pathology*, *19*, 483–492.

Rosinskin, M. J., Barmore, C. R., Dick, R. L., & Acton, J. C. (1989). Film sealant and vacuum effects on two measures of adhesion at the sealant-meat interface in a cook-in packaging system for processed meat. *Journal of Food Science*, *54*, 863–866.

Savic, Z., & Savic, I. (2002). *Sausage casings* (1st ed). Vienna, Austria: Victus, Inc.

Seiler, J.A. (1964). Tanned edible collagen casing and method of producing same. Johnson & Johnson, NJ, USA. Patent No: US 3,123,481.

Simelane, S., & Ustunol, Z. (2005). Mechanical properties of heat-cured whey protein-based edible films compared-with collagen casings under sausage manufacturing conditions. *Journal of Food Science*, *70*, E131–E134.

Su, D., Wang, C., Cai, S., Mu, C., Li, D., & Lin, W. (2012). Influence of palygorskite on the structure and thermal stability of collagen. *Applied Clay Science*, *62–63*, 41–46.

Villamonte, G., Simonin, H., Duranton, F., Cheret, R., & Lamballerie, M. D. (2013). Functionality of pork meat proteins: Impact of sodium chloride and phosphates under high-pressure processing. *Innovative Food Science & Emerging Technologies*, *18*, 15–23.

Wallace Jr., B.A. (1986). Method of joining heat shrinkable closure members. Raychem Corporation, Menlo Park, CA, USA. Patent No: US 4,586,971.

Yang, H. S., Ali, M. S., Jeong, J. Y., Moon, S. H., Hwang, Y. H., Park, G. B., & Joo, S. T. (2009). Properties of duck meat sausages supplemented with cereal flours. *Poultry Science*, *88*, 1452–1458.

Zhang, M., Ding, C., Chen, L., & Huang, L. (2014). The preparation of cellulose/collagen composite films using 1-ethyl-3-methylimidazolium acetate as a solvent. *BioResources*, *9*, 756–771.

Zhang, S., Liu, P., Chen, L., Wang, Y., Wang, Z., & Zhang, B. (2015). The effects of spheroid formation of adipose-derived stem cells in a microgravity bioreactor on stemness properties and therapeutic potential. *Biomaterials*, *41*, 15–25.

Ziolko, F.J. (1979). Method of making a tubular collagen casing. Devro, Inc., Somerville, NJ, USA. Patent No: US 4,138,503